An AI-Assisted Anti-FGFR2b Biparatopic Antibody Showed Superior Antigen Binding Affinity And Anti-Tumor Activity *In Vitro*

Zhaojun An, Li Liu, Chunqiu Xia, Peng Zhang, Yunfei Long, Shuwen Ren, Yi Li

ab.bd@xtalpi.com | Ailux Biologics Solution From XtalPi, China

Booth #306

Challenges

The structure of antigen-antibody (Ag-Ab) complex is crucial for the development of therapeutic antibodies. However, the lack of structural information for numerous targets poses significant challenges in the discovery of therapeutic antibodies, especially for new modalities and formats.

Solutions

XtalFold™, an AI-based approach for structural modeling of Ag-Ab complexes, enables the design of new antibody formats using only sequence information.
FGFR2b, which is highly expressed in various malignancies, including gastric, lung and breast cancers[1], has been recognized as a promising tumor antigen with demonstrated efficacy in clinical trials[2]. In this study, to enhance the targeted therapy, we developed a novel FGFR2b biparatopic antibody (**BpAb**) using XtalFold™.

Outcome

Based on XtalFold™ recommendations, we identified sequences that specifically bind to distinct, non-overlapping epitopes on FGFR2b, circumventing the need for traditional antibody production and epitope binning analysis. These sequences informed the design of our BpAb. Notably, the AI-designed BpAb-1, as an illustrative example, exhibited significantly higher binding affinity and superior anti-tumor efficacy in *in vitro* functional assays compared to its counterpart epitope mAbs and a clinical-stage benchmark antibody bemarituzumab (Bema).

These results highlight the effectiveness and cost-efficiency of XtalFold™ in identifying Ag-Ab binding sites and expediting the design of BpAbs with enhanced therapeutic potential.

XtalFold™ Platform: Rapidly predicted the structure of Ab-Ag complexes and recommended binding epitopes for BpAb design

The development of BpAbs generally requires mAbs targeting two distinct, non-overlapping epitopes. Traditionally, this identification process is complex and time-consuming, involving protein synthesis, epitope binning, and functional evaluations. However, Xtalfold™ bypasses this process by enabling accurate prediction of the Ag-Ab complex structure using only the sequence data as input. To illustrate, the selection of binding epitopes for anti-FGFR2b BpAbs can be significantly accelerated with XtalFold™, as outlined below.

Step 1

- Anti-FGFR2b hybridoma clones were generated using our in-house XtraDoma™ platform.
- A total of 36 **hits** were identified and sequenced from hybridoma.

Step 2

These 36 sequences were input into **XtalFold™** to predict the **structure** of the FGFR2b-Ab complex, without generating the corresponding proteins.

Step 3

- Xtalfold™ identified the binding epitopes on FGFR2b and classified into several distinct clusters. Among these clusters, two were found to be non-overlapping, containing 8 hits in cluster 1 & 2 hits in cluster 2.
- To further narrow down hits for BpAb development, we performed a comprehensive analysis and selected 4 hits from cluster 1 and 2 hits from cluster 2.

Step 4

A total of 6 BpAbs (including 2 BpAbs as negative controls (NCs)) were produced in an Fc-enhanced format, and their binding affinities were evaluated using FACS.

Step 5

To further confirm the biological superiority, BpAb-1, as an example, was assessed using a set of *in vitro* functional assays, including measuring binding affinity on cell lines with varied FGFR2b expression level, ligand (FGF-7) blockade activity, FGFR2 (Y653/654) phosphorylation, cell proliferation and ADCC activity on tumor cells. Bema, Fc-enhanced Epi-1 mAb and Epi-2 mAb were used as controls for the assays.

XtalFold™ predicted the binding sites for 36 anti-FGFR2b Ab-Ag complexes, which facilitated the design of BpAbs

a

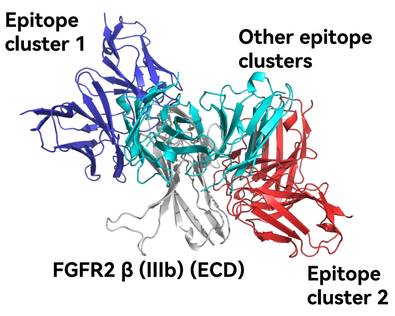

b

Epitope Cluster 1			Epitope Cluster 2		
Xtradoma™ hits	OD450	MMGBSA	Xtradoma™ hits	OD450	MMGBSA
004 (Epi-1)	3.23	-58.93	017 (Epi-2)	2.70	-45.56
020	3.09	-53.18	015	3.06	-43.28
008	2.43	-58.60	…	…	…
019	2.74	-60.48			
…	…	…			

c

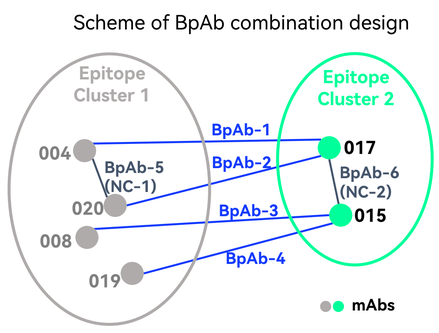

d

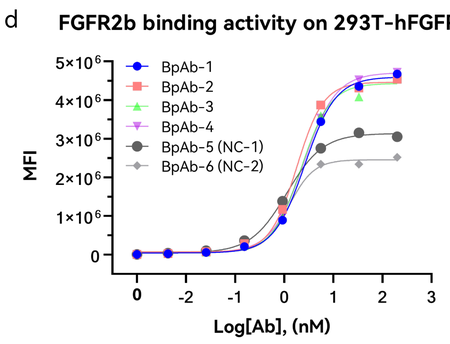

Figure 1. The epitopes of 36 anti-FGFR2b Abs were mapped onto FGFR2b and grouped into several clusters, including two distinct non-overlapping clusters (epitope clusters 1 and 2). This classification facilitated the design of BpAbs. (a). A schematic representation of the FGFR2b–Ab complex, as predicted by XtalFold™. **(b).** Computational and experimental results of anti-FGFR2b hits with two non-overlapping epitope clusters. **(c).** BpAbs design scheme**. (d).** BpAbs were generated and evaluated for their binding affinities to FGFR2b by FACS. The results indicate that BpAbs assembled across different clusters (1-4) demonstrate significantly enhanced binding affinities compared to those assembled within the same cluster (5-6, NCs).
MMGBSA: Molecular Mechanics Generalized Born Surface Area

Highlights

- Xtalfold™ accurately predicted the structures of the FGFR2b – anti-FGFR2b complex.
- FACS analysis revealed that BpAbs assembled across distinct epitope clusters exhibited higher binding affinities compared to those within the same cluster, serving as negative controls (NCs). This outcome validates the precise classification of epitope clusters by Xtalfold™
- Xtalfold™ proves to be a valuable tool for streamlining the selection of BpAb candidates, significantly expediting the design process through its reliable complex structure predictions.

REFERENCES
1. MA Krook et al. British Journal of Cancer (2021) 124:880–892;
2. Wainberg ZA, et al. Lancet Oncol. 2022;23(11):1430-1440;

Anti-FGFR2b BpAb-1 showed enhanced binding ability on SPR assay and on all the three cells with varying level of hFGFR2b expression

Sample	ka (1/Ms)	kd (1/s)	KD (M)
BpAb-1	4.74E+05	4.56E-05	9.61E-11
Epi-1 mAb	3.81E+05	1.45E-04	3.81E-10
Epi-2 mAb	3.69E+05	1.86E-04	5.05E-10
Bema	4.02E+05	1.56E-04	3.87E-10

Figure 2. In SPR assay, anti-FGFR2b BpAb-1 showed ~5-fold lower KD compared to Bema and its counterpart epitope mAbs Epi-1 and Epi-2.

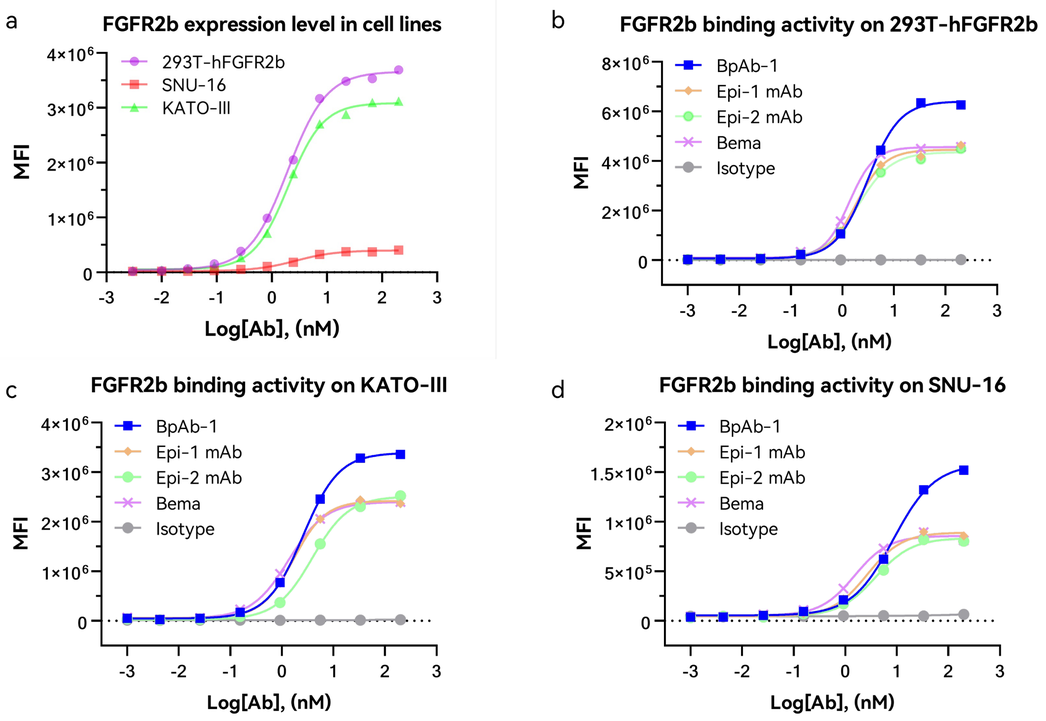

Figure 3. Anti-FGFR2b BpAb cell binding assay by FACS. (a). hFGFR2b expression levels of 3 cell lines; **(b).** Binding ability evaluation on 293T-hFGFR2b, **(c).** KATO-III, and **(d).** SNU-16.

Anti-FGFR2b BpAb-1 had stronger cytotoxicity and ADCC killing activity on SNU-16 by affecting the FGF-7 – FGFR2b signaling pathway

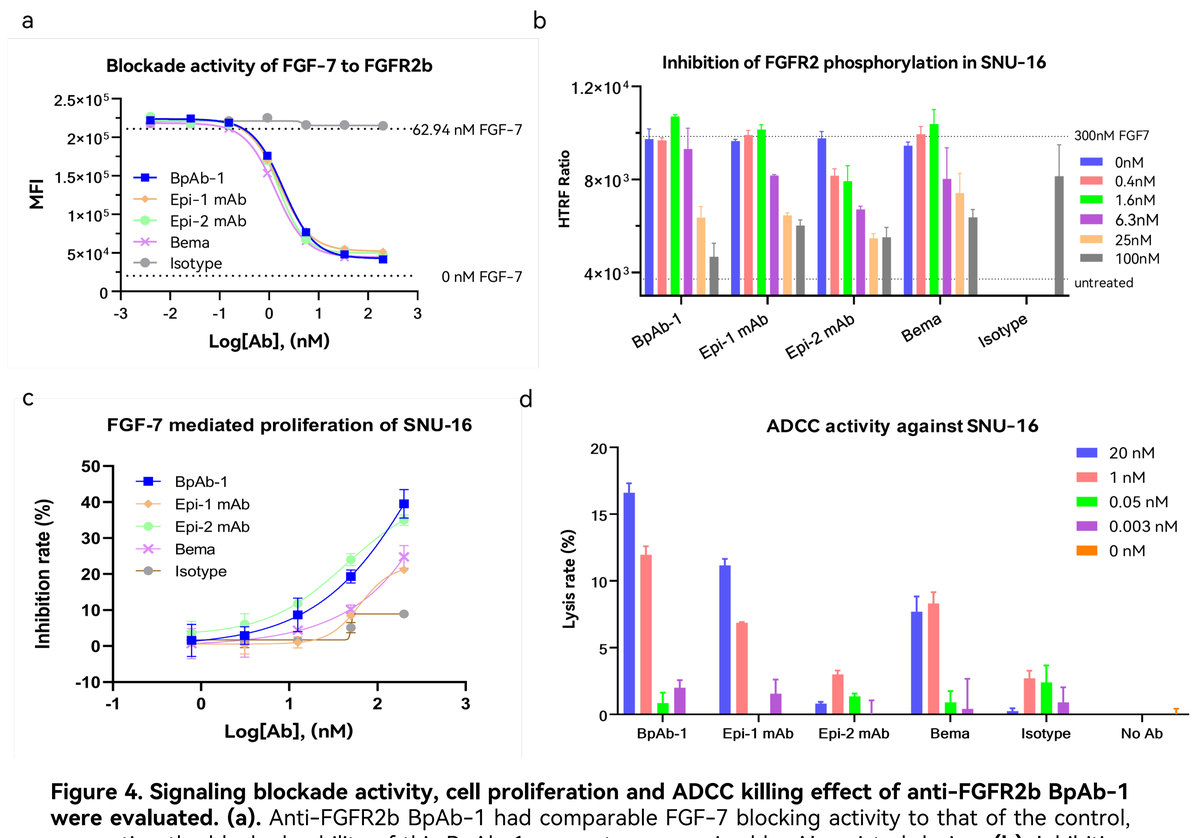

Figure 4. Signaling blockade activity, cell proliferation and ADCC killing effect of anti-FGFR2b BpAb-1 were evaluated. (a). Anti-FGFR2b BpAb-1 had comparable FGF-7 blocking activity to that of the control, suggesting the blockade ability of this BpAb-1 was not compromised by AI-assisted design. **(b).** Inhibition of FGFR2 (Y653/654) phosphorylation. **(c)**. Anti-FGFR2b BpAb-1 exhibited a significantly stronger inhibition effect on SNU-16 proliferation and **(d).** displayed more potent ADCC killing effect against SNU-16.

Discussion: Assisted by XtalFold™, a FGFR2b BpAb with superior anti-tumor activity *in vitro* was successfully developed.

This study highlighted the critical role of XtalFold™ in the design of an efficacious anti-FGFR2b BpAb. Utilizing the complex structure generated by XtalFold™, we strategically selected two mAbs with non-overlapping epitopes to construct the Fc-enhanced BpAb. Remarkbly, the entire development process of the BpAb was completed in **under two weeks**. Our research revealed that the designed anti-FGFR2b BpAb not only displayed enhanced binding affinity but also exhibited more potent anti-tumor efficacy *in vitro* by blocking the FGF7 – FGFR2b signaling pathway. (Future updates will provide insights into the performance of other BpAbs assembled across different clusters.)

Looking forward, we anticipate that XtalFold™ will emerge as a transformative tool for the early-stage antibody therapeutics discovery, including humanization, affinity maturation, pH-dependent antibody engineering, etc.. We are optimistic that our AI-driven technology will empower scientists and facilitate the exploration of macromolecular therapeutics.

Presented at PEPTALK, San Diego, CA, January 16-19, 2024
To learn more about XtalFold™, please scan the QR code.

XploreSeq™ : AI-Enhanced Antibody Discovery Platform via Immune Repertoire Next-Gen Sequencing

Ke Zhang, Bin Wei, Zenglin Pei, Shijian Ding, Yupeng Zhu, Xuemin Pan, Wenwen Cai, Xinxin Chu, Yali Wang, Shuwen Ren, Zhiwu Sun, Xingda Ye, Yi Li

ab.bd@xtalpi.com Ailux , Biologics Solution From XtalPi, China

Booth #306

ABSTRACT

With the progression of Next-Generation Sequencing (NGS) technology, remarkable strides have been made in both academia and industry concerning the study of immune repertoires. Among these advancements, the utilization of Bulk BCR sequencing, single-cell transcriptome sequencing, and single-cell BCR sequencing in combination has emerged as a potent approach for antibody discovery. These methods enable the acquisition of a vast amount of high-quality antibody sequence information from immune samples.

By leveraging sequence and/or structure-based AI algorithms, we can effectively navigate through the extensive sequence space, enabling high-throughput, multi-dimensional antibody assessment, ultimately leading to the discovery of top-tier antibodies.

Here we present XploreSeq™, XtalPi's propriety AI-enhanced NGS antibody discovery platform with remarkable adaptability, scalability, speed and quality.

Keywords: Antibody discovery, NGS sequencing, Single Cell sequencing, bulk sequencing, immune repertoire, GPCR, common light chain bispecifics, developability

PLATFORM

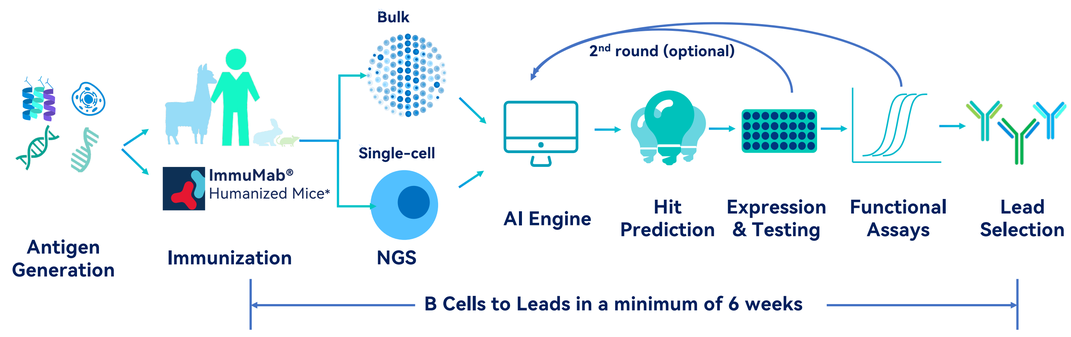

* Partnered with Immunocan®

CONCLUSION

XploreSeq™ is XtalPi's propriety AI-enhanced NGS antibody discovery platform leveraging meticulous NGS design, in-depth bioinformatics analysis, sequence and/or structure-based AI algorithms to mine the immune repertoire. It has proven success in many different antibody discovery campaigns. The immune repertoire data from NGS also has great potential in enabling downstream antibody engineering.

CASE STUDY 1: Repertoire Discovery & Iterative Selection

Round 1

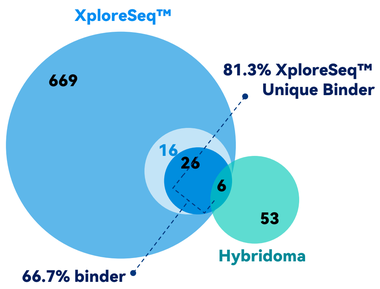

In an internal project, XploreSeq™ predicted 717 binders, from which 48 were chosen for round 1 expression and testing. 66.7% (32/48) were confirmed to be binders, and only 18.6% (6/32) binders overlap with hybridoma hits.

Round 2

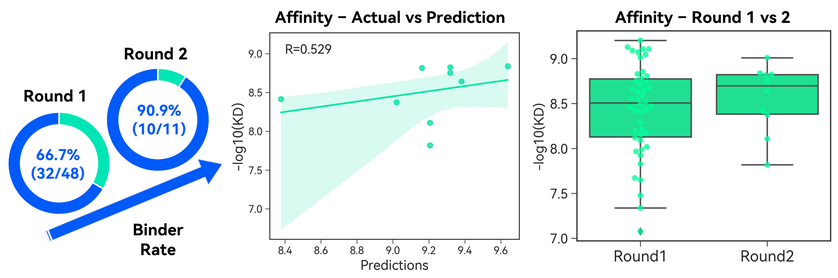

Based on round 1 data, binder and affinity prediction models were trained and used for round 2 antibody selection. Binder rate in round 2 was improved from 66.7% to 90.9%. Correlation between actual and predicted affinity was at R=0.529. 4/10 of round 2 sequences were within or close to picomolar range level affinity.

CASE STUDY 2: XploreSeq™ vs. Heuristic Method

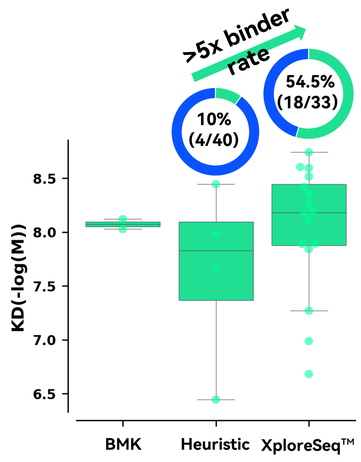

To demonstrate the efficacy of the XploreSeq™ platform for obtaining binders from immune repertoires, we performed a side-by-side comparison with a heuristic method where a weighted sum of reads, SHM, and clonotype frequencies were used as a score for picking hits in an in-house project.

XploreSeq™ achieved a **4 fold increase in identifying binders** than Heuristic methods with an overall higher affinity.

CASE STUDY 3: GPCR Rare Binder Discovery

1,848,574 Unique VH Sequences

19,235 VH Clonotypes

3 Animal batches

6 NGS Datasets

4,220 VL Clonotypes

1,809,574 Unique VL Sequences

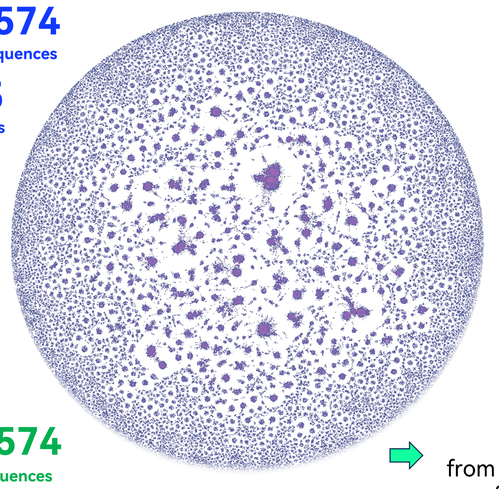

Total BCR Raw Repertoire

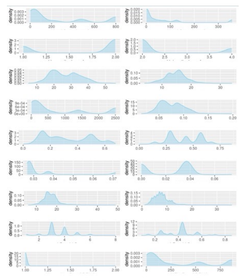

100+ features
from single cell & bulk NGS + feature engineering

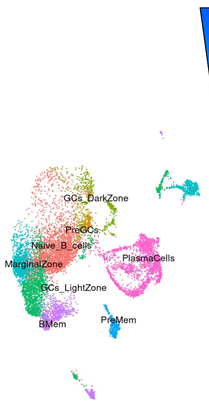

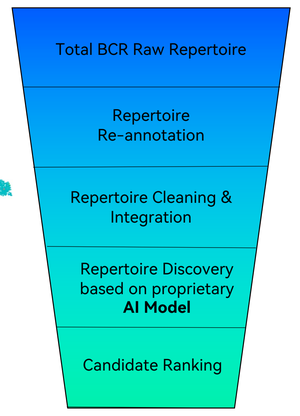

76 predicted binders
From 66 clonotypes
72 unique HCDR3

20 selected mAbs Expressed & Tested
11/20 binding & blocking

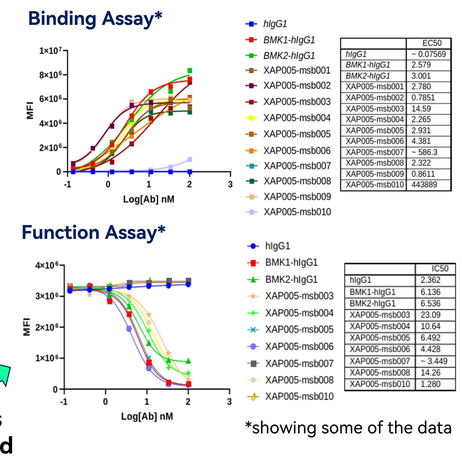

	EC50
hIgG1	~ 0.07569
BMK1-hIgG1	2.579
BMK2-hIgG1	3.001
XAP005-msb001	2.780
XAP005-msb002	0.7851
XAP005-msb003	14.59
XAP005-msb004	2.265
XAP005-msb005	2.931
XAP005-msb006	4.381
XAP005-msb007	~ 586.3
XAP005-msb008	2.322
XAP005-msb009	0.8611
XAP005-msb010	443889

	IC50
hIgG1	2.362
BMK1-hIgG1	6.136
BMK2-hIgG1	6.536
XAP005-msb003	23.09
XAP005-msb004	10.64
XAP005-msb005	6.492
XAP005-msb006	4.428
XAP005-msb007	~ 3.449
XAP005-msb008	14.26
XAP005-msb010	1.280

*showing some of the data

XploreSeq™
XtraDoma™
XpeedPlay™

Additional data from the same campaign

Hit Amplification
30 selected mAbs
Natural Sequences
PTM motifs mitigated
Expressed & Tested

Binding
23 human hits
24 cyno hits
20 human-cyno hits

Function Assay 1
8 hits

Function Assay 2
4 hits

Lead Confirmation
ongoing

CASE STUDY 4: Immune Repertoire Data Enabled Antibody Engineering

Case 1: Common Light Chain Bispecific Antibodies

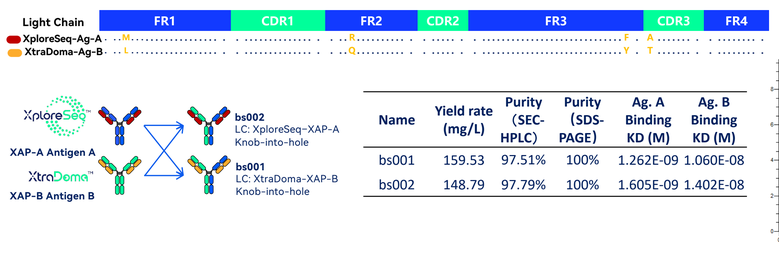

Name	Yield rate (mg/L)	Purity (SEC-HPLC)	Purity (SDS-PAGE)	Ag. A Binding KD (M)	Ag. B Binding KD (M)
bs001	159.53	97.51%	100%	1.262E-09	1.060E-08
bs002	148.79	97.79%	100%	1.605E-09	1.402E-08

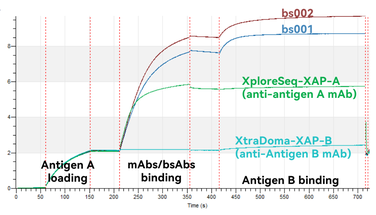

XploreSeq™ collects lights chain sequences in the millions, which makes it uniquely positioned to search for common light chains from multiple repertoires. In this case, XploreSeq™ was able to identify a similar light chain in the antigen A repertoire with a hit identified by our XtraDoma™ (hybridoma) platform for antigen B. We then built two common LC bispecific antibodies based on this common sequence. Both molecules **expressed well, showed high purity, and bound both targets as intended.**

Case 2: Post Translational Modification Removal

	CDR2	
	50 51 52 52A 53 54 55 56 57 58 59 60 61 62 63 64 65	
mAb048	L I Y P G **N G** Y T N Y **N G** R F K V	
msb017	L I Y P G **G** G Y T N Y N **E** R F K V	NGS-informed
msb018	L I Y P G **T** G Y T N Y N **V** R F K V	NGS+CADD+Rational

Name	Source	VH PTM sites	ka (1/Ms)	kd (1/s)	KD (nM)
BMK	Commercial	0	4.55E+05	8.87E-04	1.95
mab048	hybridoma	2	5.15E+05	1.42E-04	0.275
msb017	NGS-informed	0	8.23E+05	6.00E-04	0.729
msb018	NGS+CADD+rational	0	7.05E+05	2.08E-04	0.294

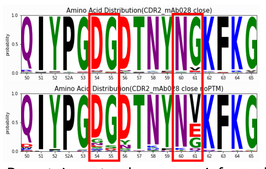

Repertoire natural sequence informed amino acid substitution suggestion

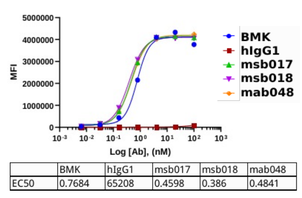

	BMK	hIgG1	msb017	msb018	mab048
EC50	0.7684	65208	0.4598	0.386	0.4841

In an internal project, a functional lead, antibody mab048, was derived from hybridomas. Two deamidation sites with high risk, assessed by XcelDev™ PTM algorithm, were identified on its HCDR2. By combining the sequence space obtained through XploreSeq™, CADD calculations, and the expertise of antibody engineering specialists, modifications were made resulting in two engineered antibodies, msb017 and msb018. Modifications **eliminated the PTM sites while retaining affinity and cellular activity for both engineered antibodies.**

Presented at PEPTALK, San Diego, CA, January 16-19, 2024

To learn more about XploreSeq™, please scan the QR code.

XrossXeven™: AI-powered GPCR Protein Antigen *De Novo* Design

Yali Zhou, Chunqiu Xia, Xinming Li, Sijin Wu, Yunfei Long, Zhiwu Sun, Yi Li

ab.bd@xtalpi.com | Ailux Biologics Solution From XtalPi, China

Booth #306

Full-length GPCR Antigen Preparation

Opportunities

Preparing pure GPCR antigens with native conformation is crucial for the isolation of therapeutic antibody molecules.

Because of the large hydrophobic transmembrane domains and limited exposure epitopes, various antigen formats are developed for GPCR antibody discovery.

Purified protein antigens, as opposed to DNA and overexpressed cells, usually induce superior immunization effects and allow for exclusion of impurities, which will help improve the isolation of target-specific antibodies.

Challenges

Due to the low expression level on cell membranes, low solubility and stability of expressed proteins, and complex and time-consuming purification methods, full-length protein antigens are rarely used in antibody discovery[1].

Solutions: AI-Powered *de novo* GPCR Antigen Design

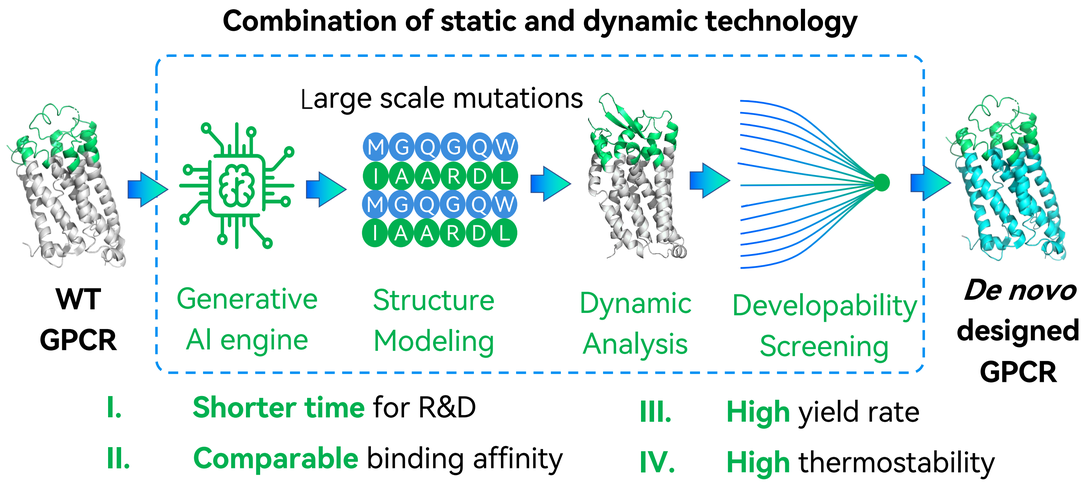

Fig. 1. Schematic diagram of AI-powered *de novo* GPCR antigen design workflow.

Step 1

A generative AI model were trained using all available data from solved GPCR and non-GPCR structures in the Protein Data Bank (PDB).

Step 2

The wild-type GPCR structure was constructed, and potential epitopes were analyzed.

Step 3

The generative AI model were employed to generate new sequences with large-scale mutations in the non-epitope transmembrane domains.

Step 4

The structures of the new GPCRs were modeled and their structural stability were analyzed using molecular dynamics (MD) simulations.

Step 5

The *de novo* designed GPCR sequences were obtained for wet-lab verification after conducting developability screening.

Result: *In-silico* Screening & Generation of GPCR A Sequences

Over 160,000 unique sequences that preserved the pointed epitope of GPCR A were generated. Following sequence rationality screening, approximately 10,000 sequences were subjected to structural modeling, with 100 of them undergoing dynamic analysis based on several criteria. Ultimately, 15 sequences were selected for expression and functional verification. This entire process was completed within a span of **5 weeks**.

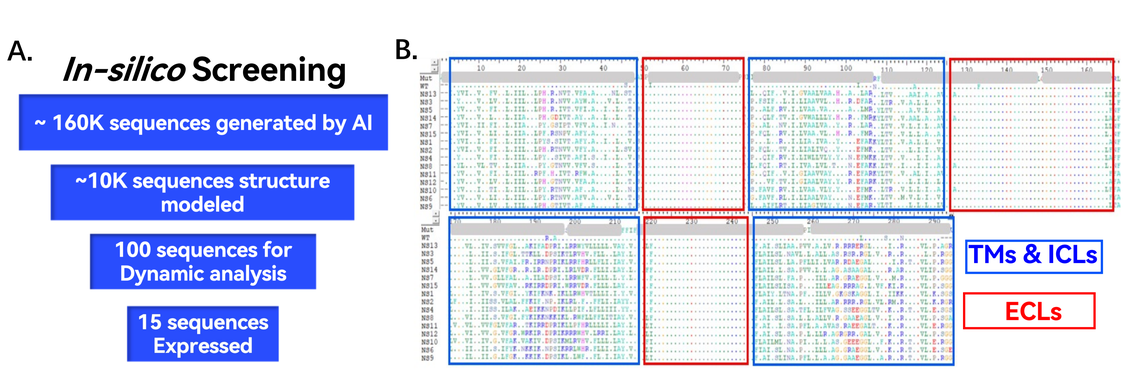

Fig. 2. (**A**) The *in-silico* screening steps of 15 GPCR A new sequences generation.
(**B**) sequence comparison (without N terminal residues) with wildtype and mutant in published paper. About **53.2%-69.7%** of residues in transmembrane domains and intracellular loops were replaced

Result: Wet-lab Evaluation on AI Generated GPCR A Novel Protein

All 15 sequences, along with the control (mutant from a published paper), were expressed in an insect system. Out of the 15 sequences generated, 13 (**86.7%**) exhibited expression on the cell membrane, and 11 (**73.3%**) demonstrated binding affinity to the known GPCR A antibody.

i. Successful expression of antigen with high yield & biological activity comparable to the control.

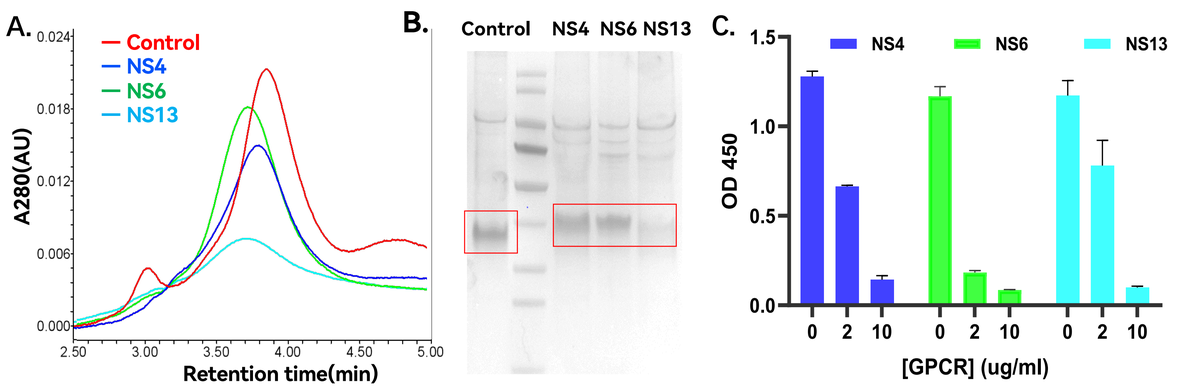

Fig. 3. (**A**) SEC and (**B**) SDS-PAGE results of new sequences 4,6,13 (NS4, NS6, NS13) and control protein purified by DDM. (**C**) Binding ELISA results of NS4, NS6, and NS13 compete binding with GPCR A antibody against control protein in different concentrations.

ii. Enhanced thermostability of *de novo* GPCRs compared to the control

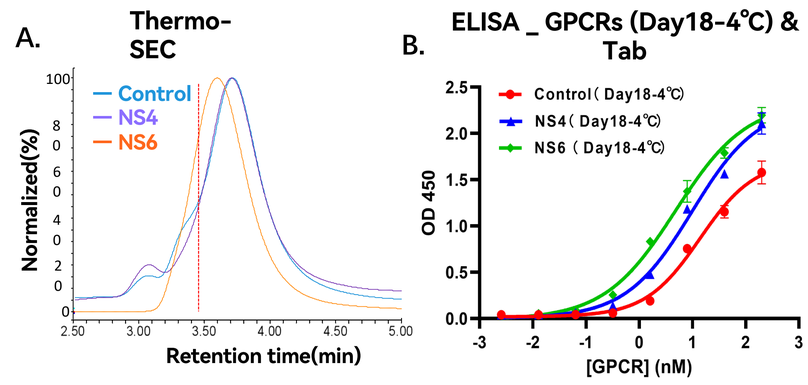

Fig. 4. (**A**) Normalized thermo-SEC results for NS4, NS6, and control after heating at 40 ℃ for 10 min.

(**B**) ELISA binding affinity results for GPCR proteins stored at 4℃ for 18 days.

iii. Comparable immune effect to conventional overexpressed cells or DNA antigens.

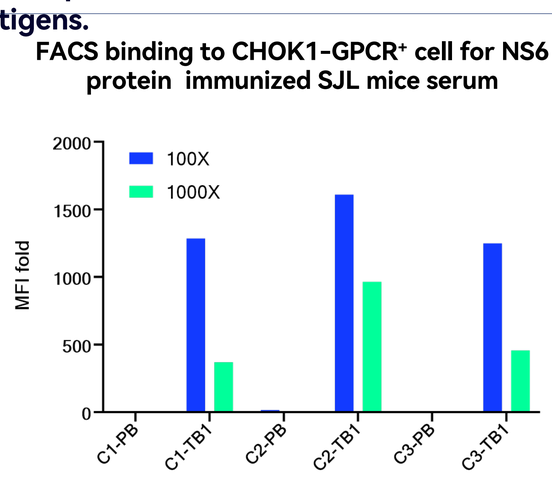

Fig. 5. Serum titer of SJL mice immunized with NS6 nanodisc protein twice, as measured by FACS.

PB: primary blood.
TB: test blood.

Conclusion: AI-generated GPCR protein antigens with excellent properties

We have developed an AI-driven, computationally assisted solution that rapidly generates high-quality GPCR protein antigens, with demonstrated excellent homogeneity, high yield rates, comparable binding affinity and immune response.

Our innovative dry-lab screening and generation of GPCR A sequence was completed within a span of 5 weeks, which significantly reduced the time required for GPCR protein optimization.

This approach offers a novel perspective on *de novo* protein antigen design for antibody discovery, with the potential to revolutionize the field of GPCR-targeted therapeutics.

References

1. Ju MS, Jung ST. Antigen design for successful isolation of highly challenging therapeutic anti-GPCR antibodies. *Int J Mol Sci.* 2020 Nov 3;21(21):8240.

XtalFold™ : An antibody-antigen/protein-protein complex structure prediction algorithm with unprecedented accuracy to accelerate therapeutics development

Chunqiu Xia, Chuheng Liang, Yihang Zhou, Yunfei Long*, Yi Li

ab.bd@xtalpi.com | Ailux, Biologics Solution From XtalPi, China

Booth #306

The Problem: Predicting the structure of antigen-antibody complexes is a critical challenge

While AlphaFold2 has shown remarkable success in predicting protein monomer structures, accurately predicting the structure of protein complexes remains a challenge.

AlphaFold-Multimer is currently the most renowned algorithm for predicting protein complex structures, but its performance in determining the structure of antigen-antibody complexes remains suboptimal.

Several existing methods, such as IgFold[3], OmegaFold[4], and ESMFold[5], can predict antibody structures, but not antigen-antibody complexes.

To address this limitation, we propose **XtalFold™, a novel approach capable of predicting antigen-antibody complex structures with high accuracy and probability**.

The Solution: An AI-driven approach named XtalFold™ for effective antigen-antibody complex structure prediciton

Recent literature[6] has utilized a rigorously curated test set from the Protein Data Bank (PDB) to assess the performance of AlphaFold-Multimer in predicting antigen-antibody complex structures.

To benchmark the performance of both XtalFold™ and AlphaFold-Multimer, we selected a fair test set (N=39) comprising newly released structures that are **NOT** included in the training dataset of both AlphaFold-Multimer and XtalFold™, and are **NOT** similar in sequence or structure to the training set.

Additionally, we incorporated a structural confidence (SC) score as a filter into XtalFold™ to further enhance prediction quality. The effectiveness of this filter was compared with AlphaFold-Multimer's pLDDT metric.

The PDB IDs and chain names of the test set (N=39)

7VNB_AB, 7E53_BA, 7ANQ_BA, 7NFQ_CA, 7NFR_BA, 7NX0_DC, 7AR0_BA, 7AQY_CB, 7DAA_HLA, 7L6V_BA, 7T5F_CA, 7T5F_ED, 7L6V_DA, 7S11_IMD, 7M1H_GA, 7L6V_CA, 7L6V_FA, 7M1H_FA, 7VUX_HLA, 7M1H_EA, 7LZP_ED, 7NA9_DA, 7PS6_HLE, 7E72_CDF, 7PS4_HLE, 7PS2_HLG, 7PS0_HLE, 7Q0G_ABE, 7MZJ_HLA, 7MZK_NMB, 7BNV_HLA, 7MZM_HLA, 7N4J_HLA, 7L0L_HLBA, 7Q0I_HLC, 7NX3_BCF, 7L7R_BAG, 7L7R_DCG, 7BBJ_HLA.

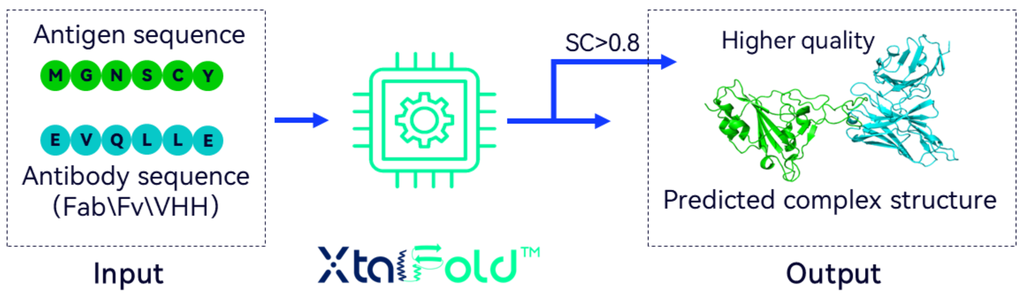

***Fig. 1**. Schematic diagram of XtalFold™. The input for this algorithm requires only the antigen and antibody sequences (VHH, Fv, or Fab), and the output generated is the antigen-antibody complex structure. Additionally, we can use SC as an effective filter to significantly improve the quality of prediction results.*

Conclusion: XtalFold™ has high success rate for Ab-Ag complex structure prediction

We have successfully developed an AI-driven solution capable of predicting the complex structure of antigen-antibody with higher probability and accuracy, relying solely on sequence information.

XtalFold™ demonstrates significant potential for predicting protein-protein and protein-peptide complex structures, as well as other related scenarios.

This breakthrough paves the way for numerous downstream applications, including antibody engineering, epitope identification, functional elucidation, and *de novo* design, *etc.*.

Assessment Results: XtalFold™ outperforms AlphaFold-Multimer after qualitative and quantitative evaluation with a fair test set.

XtalFold™ exhibits a superior ability to provide precise modeling for these complexes. In contrast, AlphaFold-Multimer fails to accurately model several typical antigen-antibody or protein-protein complex structures.

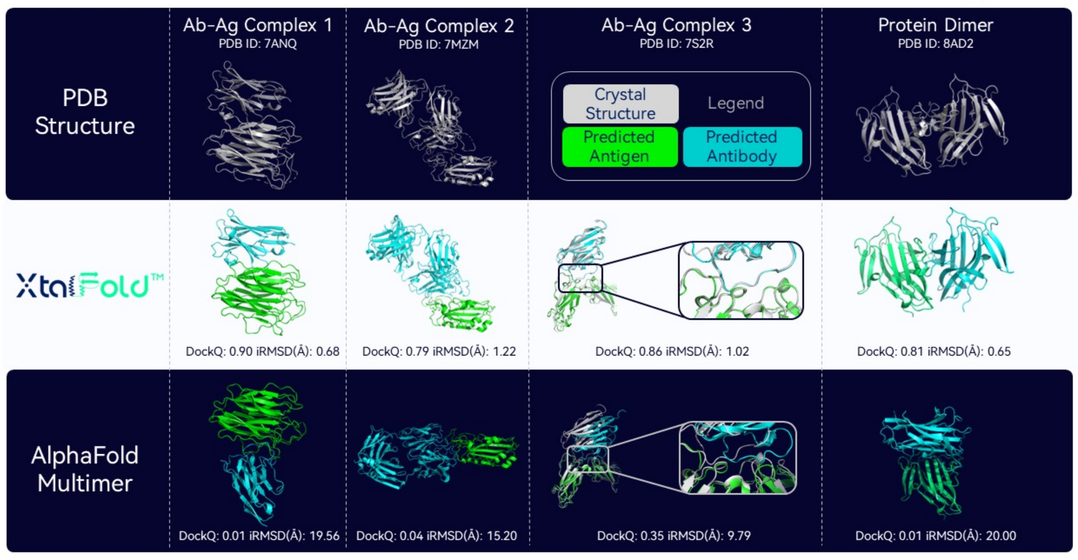

***Fig. 2**. Visualization of typical predicted complex structures, comprising antigen-antibody complexes and protein-protein complexes. DockQ: higher values indicate better predictions; DockQ ≥ 0.80 is considered high-quality, 0.8 > DockQ ≥ 0.49 is considered medium-quality, 0.49 > DockQ ≥ 0.23 is considered acceptable-quality, and 0.23 > DockQ ≥ 0 is considered incorrect prediction. iRMSD (interface RMSD): lower values indicate better predictions; ≤1.50 is considered high-quality prediction.*

XtalFold™ significantly outperforms AlphaFold-Multimer across all four performance metrics.

As depicted in **Fig. 3**, the success rate of correctly modeled structures by XtalFold™ is 192% that of AlphaFold-Multimer. If filtering out only 25.6% of structures with low SC, the modeling accuracy of XtalFold™ is further improved, reaching 250% of AlphaFold-Multimer's performance.

Moreover, the interface modeling quality of XtalFold™ is also exceptionally high, achieving 440% of AlphaFold-Multimer's performance after SC filtering.

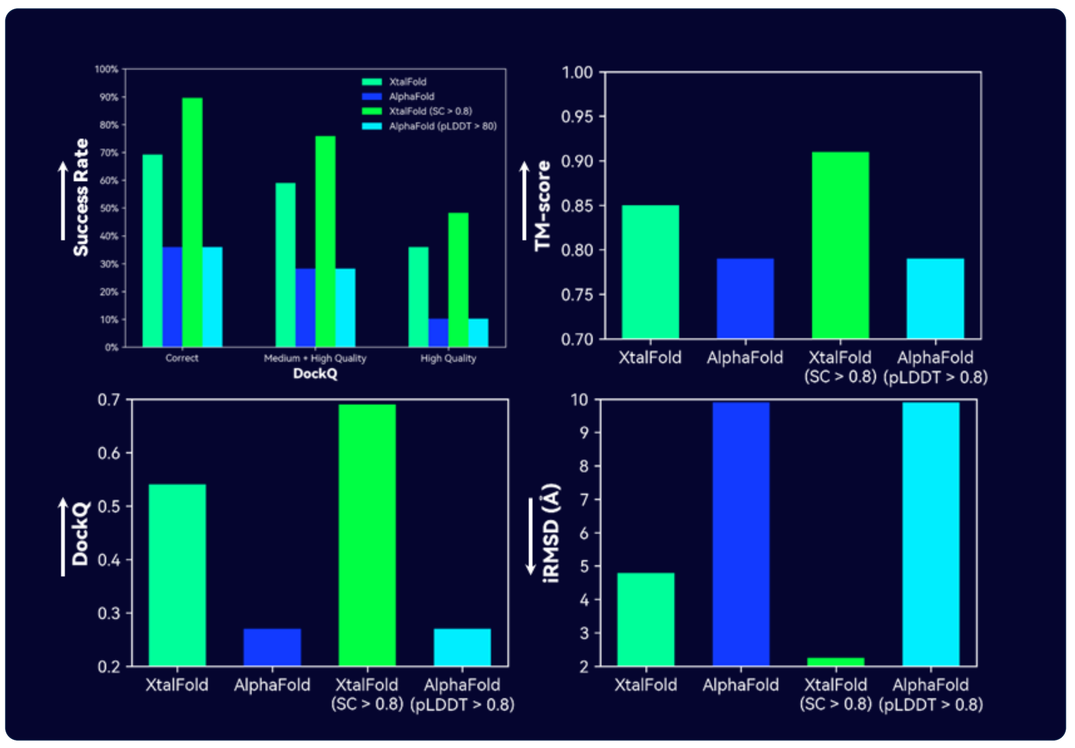

***Fig. 3**. Statistical results of XtalFold™ and AlphaFold-Multimer(N=39). DockQ ≥ 0.23 is considered correct prediction (including acceptable, medium and high quality). The average, standard deviation, median, minimum, and maximum values for the total amino acid length of antigens and antibodies in this test set are 581.6, 128.7, 553, 330 and 952, respectively.*

Reference

[1] Jumper J, Evans R, Pritzel A, et al. Highly accurate protein structure prediction with AlphaFold[J]. Nature, 2021, 596(7873): 583-589.
[2] Evans R, O'Neill M, Pritzel A, et al. Protein complex prediction with AlphaFold-Multimer[J]. biorxiv, 2021: 2021.10. 04.463034.
[3] Ruffolo J A, Chu L S, Mahajan S P, et al. Fast, accurate antibody structure prediction from deep learning on massive set of natural antibodies[J]. Nature communications, 2023, 14(1): 2389.
[4] Wu R, Ding F, Wang R, et al. High-resolution de novo structure prediction from primary sequence[J]. BioRxiv, 2022: 2022.07. 21.500999.
[5] Lin Z, Akin H, Rao R, et al. Evolutionary-scale prediction of atomic-level protein structure with a language model[J]. Science, 2023, 379(6637): 1123-1130.
[6] Yin R, Pierce B G. Evaluation of AlphaFold Antibody-Antigen Modeling with Implications for Improving Predictive Accuracy[J]. bioRxiv, 2023: 2023.07. 05.547832.

Presented at PEPTALK, San Diego, CA, January 16-19, 2024
To learn more about XtalFold™, please scan the QR code.

An AI-Assisted Selective CD16A-targeting NK Cell Engager Showed Superior Anti-tumor Activity *In Vitro*

Huilin Li, Ke Zhang, Bin Wei, Xingda Ye, Quan Yu, Shuwen Ren, Yi Li

ab.bd@xtalpi.com | Ailux Biologics Solution From XtalPi, China

Booth #306

Opportunities

NK cell bispecific antibodies represent a promising new approach to cancer immunotherapy by harnessing the power of the immune system to recognize and kill cancer cells more effectively.

The development of an NK cell engager (NKCE) that selectively targets CD16A but not CD16B holds promise as a potential cancer immunotherapy, without inducing CD16B-mediated adverse effects on neutrophils.

Challenges

Due to the mere 2-amino-acid difference in the extracellular domain between CD16A and CD16B, obtaining antibodies with higher specificity poses a significant challenge.

Conclusions

In this study, our XploreSeq™ platform rapidly generated several antibodies specifically targeting CD16A within just 8 weeks, utilizing AI-assisted large repertoire exploration, evaluation, and hit recommendations. Then, NK bispecific antibodies targeting EGFR tumors were generated by hit Msb021 in different formats.

In particular, BsAb03 and BsAb04 exhibited significantly higher NK activation and NK-mediated killing efficacy on a tumor cell line with moderate EGFR expression and showed a comparable cytokine release panel compared to front runner AFM24, which is an EGFR x CD16A bispecific antibody and currently in phase 1.

XploreSeq™ Platform: Rapid discovery of CD16A-specific antibodies

AI-empowered Antibody Discovery Platform XploreSeq™ were utilized for high-throughput hit identification from 2 mice immunized with CD16A.

The streamlined process, from next-generation sequencing to AI-powered evaluation, enables the rapid identification of antigen-specific antibodies for this NKCE campaign.

Step 1

Integrating single-cell and bulk NGS to sequence millions of B-cell receptors (BCRs), dramatically expanded the explored antibody sequence space.

Step 2

A rigorous bioinformatics pipeline assured high-quality BCR calling and data integrity at both cellular and sequence levels.

Step 3

AI-driven models, employing self-supervised and supervised learning, processed this data to evaluate antibody candidates for binding, affinity, function and developability.

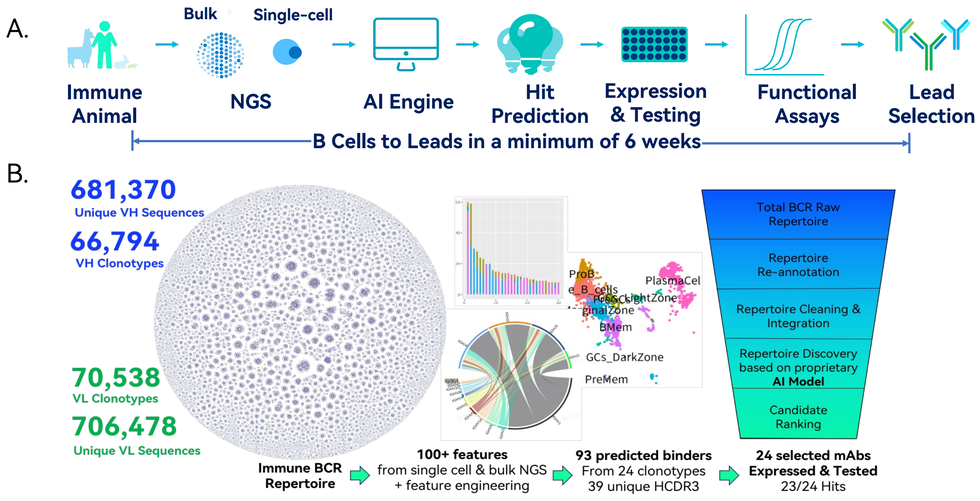

Figure 1. A. XploreSeq™ Platform Workflow; B. XploreSeq™ for NKCE Discovery

NKCE Platform: Engineering various formats of BsAbs with a high yield

In the development of the XtalPi NKCE platform, we engineered BsAbs to dual-target EGFR, which is expressed on tumor cells, and CD16A, which bridges and activates NK cells. The bivalent antibody arms, in either scFv or Fab form, were engineered into symmetrically structured, Fc-silenced IgG1 bispecific antibodies. Subsequently, the BsAbs were produced and purified in various formats with a high yield.

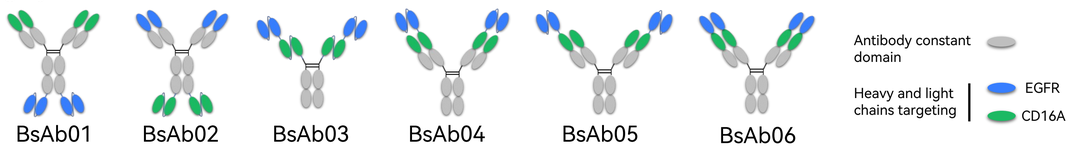

Msb021 exhibited a 10-fold higher affinity for specifically targeting CD16A compared to AFM24 anti-CD16A arm, while not interacting with CD16B

A. SPR binding kinetics of Msb021 interaction with human CD16A-V158 and CD16A-F158 variants

CD16A binding moiety	hCD16A-V158				hCD16A-F158			
	ka(1/Ms)	kd(1/s)	KD(M)	KD Fold	ka(1/Ms)	kd(1/s)	KD(M)	KD Fold
Msb021	1.70E+06	3.36E-03	1.98E-09	10.9	1.85E+06	2.94E-03	1.59E-09	10.8
AFM24 anti-CD16A arm	3.18E+05	6.83E-03	2.15E-08	/	3.52E+05	6.05E-03	1.72E-08	/

KD Fold = $KD_{(AFM24\ anti\text{-}CD16A\ arm)}$ / $KD_{(Msb021)}$

B. SPR binding kinetics of Msb021 interaction with human CD16B-NA1 and CD16B-NA2 variants

CD16A binding moiety	hCD16B-NA1			hCD16B-NA2		
	ka(1/Ms)	kd(1/s)	KD(M)	ka(1/Ms)	kd(1/s)	KD(M)
Msb021	N.B	N.B	N.B	N.B	N.B	N.B
AFM24 anti-CD16A arm	N.B	N.B	N.B	N.B	N.B	N.B

N.B = No Binding

Figure 2. Evaluation of Msb021 binding kinetics by Surface Plasmon Resonance (SPR) Assay

NK bispecific antibodies showed a high binding affinity profile for both EGFR and CD16A overexpressed cells

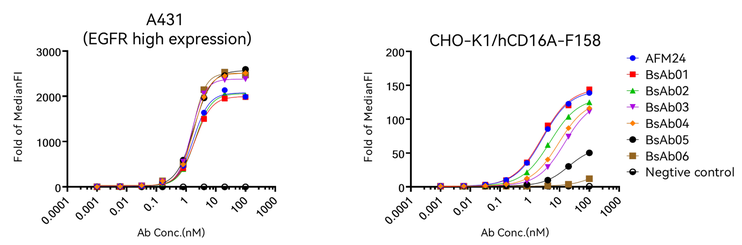

Figure 3. Binding affinities of NK BsAbs against EGFR and CD16A, which were individually evaluated on cells overexpressing EGFR and CD16A by flow cytometry (FACS) .

BsAb03 and BsAb04 showed significantly stronger activities in activating NK cells and promoting NK-mediated cytotoxicity, particularly against HT-29 cells with moderate EGFR expression, in comparison to AFM24

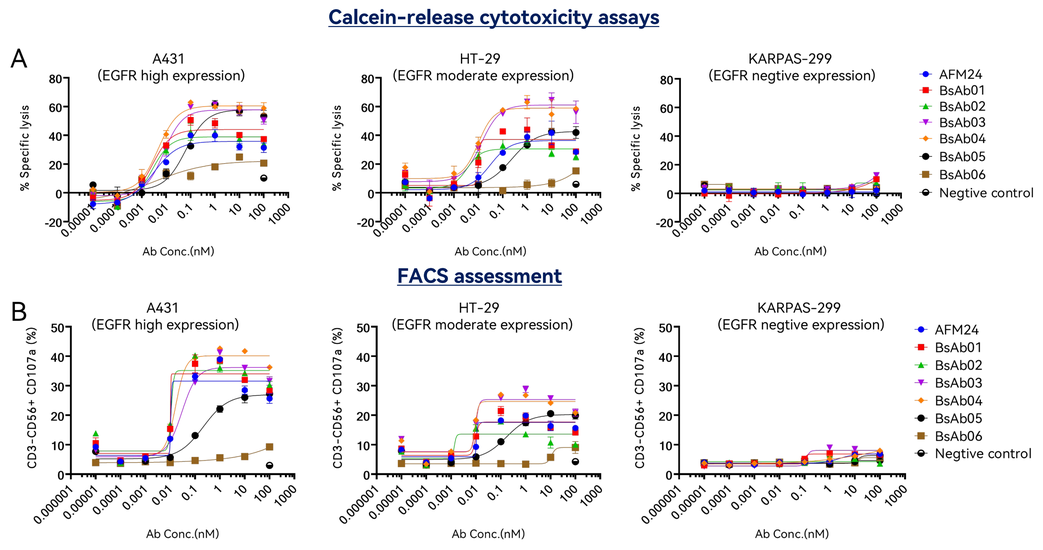

Figure 4. NK activation and NK-mediated cytotoxicity against tumor cells exhibiting high, moderate and negative EGFR expression levels were assessed in the presence of EGFR x CD16A bispecific antibodies. NK-mediated cytotoxic effect on tumor cells was assessed using calcein-release cytotoxicity assays, with human peripheral blood mononuclear cells (PBMCs) serving as effector cells at an effector-to-target (E:T) ratio of 50:1 (**A**). CD107a, the cell surface marker of activated NK cells was assessed by FACS (**B**).

BsAb03 and BsAb04 showed comparable release levels of TNFα, and IL-6 as compared to AFM24

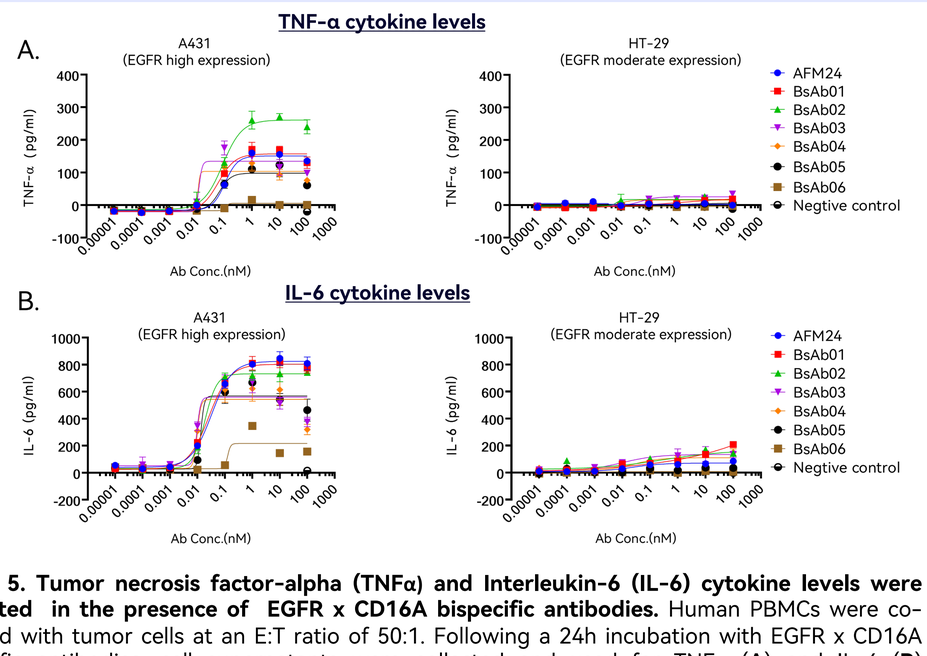

Figure 5. Tumor necrosis factor-alpha (TNFα) and Interleukin-6 (IL-6) cytokine levels were evaluated in the presence of EGFR x CD16A bispecific antibodies. Human PBMCs were co-cultured with tumor cells at an E:T ratio of 50:1. Following a 24h incubation with EGFR x CD16A bispecific antibodies, cell supernatants were collected and used for TNFα (**A**) and IL-6 (**B**) detection.

Discussion: Assisted by XploreSeq™, our NKCE platform engineered BsAbs with superior anti-tumor activity *in vitro*.

XploreSeq™ Platform

We utilized the XploreSeq™ for anti-CD16A antibody generation, obtaining over 680,000 heavy chain sequences and 700,000 light chain sequences.

From these, 93 candidate antibodies were identified, and 24 were selected for expression and evaluation. **A remarkable 95.8% (23/24) were confirmed as binders.**

The hit antibody Msb021, which specifically targets CD16A but not CD16B, was generated in just **8 weeks** and demonstrated a **10-fold higher** affinity for human CD16A in an SPR assay.

XploreSeq™ enables the rapid identification of antigen-specific antibodies for this NKCE campaign.

NKCE Platform

Following engineering with Msb021, the EGFR x CD16A bispecific antibodies demonstrated significantly enhanced NK-mediated efficacy in an EGFR-dependent manner.

Compared to AFM24, BsAb03 and BsAb04 exhibited significantly enhanced NK activation activity and NK-mediated cytotoxicity, particularly against HT-29 cells with moderate EGFR expression. This suggests our NKCEs may offer an opportunity to target tumor types even with moderate EGFR expression.

Our NKCEs offer a robust bispecific platform featuring **a diverse range of format options, potent NK-mediated efficacy, and an acceptable cytokine release profile**.

In future, we will leverage the strengths of our AI and biology experimental teams to further develop the NKCE platform. This will entail improving *in vivo* drug efficacy assessment, druggability evaluation and modification, and other aspects to progress the NKCE platform's products towards clinical applications.

Presented at PEPTALK, San Diego, CA, January 16-19, 2024

To learn more about XrossXeven™, please scan the QR code.